Supporting Information

Boosting the Thermoelectric Performance of SnTe through Localized van der Waals Gaps construction and Configurational-Entropy Engineering

Mengqi Li[a], Hu Zhang[b, *], Fudong Zhang[a], Weishuai Wang[a] , Mingrui Zhang[a], Baopeng Ma[a], Beiquan Jia[a], Yalin Shi[a], Zupei Yang[a, *], Di Wu[a, *]

[a] Key Laboratory for Macromolecular Science of Shaanxi Province and Shaanxi Key Laboratory for Advanced Energy Devices, School of Materials Science and Engineering, Shaanxi Normal University, Xi'an, 710119, China

[b] School of Physics and Information Technology, Shaanxi Normal University, Xi'an, Shaanxi, 710119, China.

*Corresponding addresses: zhanghu274@snnu.edu.cn (H. Zhang), yangzp@snnu.edu.cn (Z. Yang), wud@snnu.edu.cn (D. Wu)

Experimental section

1. Synthesis

This work uses conventional melting methods to synthesize high quality polycrystalline ingots of $(SnTe)_{0.85}(Ag_{1-\delta}Sb_{1+\delta}Te_{2+\delta})_{0.15}$ (δ = 0, 0.1, 0.2, 0.3) and $(Sn_{1-x-y-z-w}Pb_xGe_yNd_zIn_wTe)_{0.85}(Ag_{0.8}Sb_{1.2}Te_{2.2})_{0.15}$ (x = 0.15, y = z = w = 0; x = 0.15, y = 0.05, z = w = 0; x = 0.15, y = 0.05, z = 0.005, w = 0; x = 0.15, y = 0.05, z = w = 0.005). Stoichiometric amounts of highly pure Sn (99.99%, Aladdin), Ag (99.99%, Alfa Aesar), Sb (99.99%, Aladdin), Te (99.99%, Aex), Ge (99.99%, Alfa Aesar), Pb (99.99%, Aladdin), In (99.99%, Aladdin), Nd (99%, Aex) elements were mixed and sealed in carbon-coated quartz tubes under a vacuum of ~ 10^{-4} Pa. The raw materials were heated up to 673 K firstly and held at this temperature for 2 hours, then heated to 1273 K and held for another 18 hours, then quenched in cold water and further annealed at 873 K for 48 h and furnace cooled to room temperature. Afterwards, the as-obtained ingots were hand milled to fine powders by a mortar and pestle. The obtained powders were subsequently pressed into pellets with a spark plasma sintering (SPS, LABOX-212) method; the sintering temperature, holding time, and uniaxial pressure were 773 K, 5 minutes and 50 MPa, respectively. The obtained pellets were cut into 2 × 2 × 12 mm^3 cuboids for electrical transport measurements and 6 × 6 × 2 mm^3 cubic pellets for thermal expansion coefficient measurements.

2. Characterization

The crystal structure of the sample was characterised using an X-ray powder diffractometer (MiniFlex 600, Rigaku). The test parameters are set as: Cu Kα radiation source (λ = 1.5418 Å, 40 kV, 40 mA), with a scanning rate of 10° min^{-1} from 2θ = 20° to 80°. The scanning range of 2θ was 20-80° with a scanning speed of 6°/min. Scanning electron microscope (SEM, SUB8020, Japan) equipped with energy dispersive spectroscopy (EDS) was used to detect its microstructure and corresponding elements distribution at micron-scale level. Transmission electron microscopy (TEM), Cs-corrected STEM-HAADF and energy dispersive X-ray mapping (EDX) experiments were performed using a FEI Titan Themis 60-300 kV microscope equipped with a

Super-X detector and operating at 300 kV. Followed strain analysis of the STEM HAADF images was performed by using the commercial Geometric Phase Analysis package by HREM Research.

3. Measurement

The Seebeck coefficient S and electrical conductivity σ of the materials were measured under a micro-helium atmosphere using a commercial instrument (ADVANCE RIKO ZEM-3, Japan). The experimental error for each measurement was expected to be within 5%. Thermal conductivity is calculated using the formula $\kappa_{tot} = D\rho C_p$, where D, ρ, and C_p are the thermal diffusion coefficient, mass density, and specific heat capacity, respectively. The thermal diffusion coefficient (D) was measured using a thermal expansion instrument (NETZSCH, LFA467, Germany). The sample density ρ was measured using the Archimedes drainage method. The specific heat capacity (C_p) of the sample is calculated using the Dulong-Petit law[1], that is $Cp = \frac{3RN}{M}$, where N is the number of atoms in the compound; R is the gas constant; M is the relative molecular mass of the compound. The room temperature carrier concentration and carrier mobility of the material were measured using the Lake Shore 8400 Hall effect measurement system.

4.Two-Kane band model (TBK) simulations

In our calculations of Pisarenko curves for SnTe, two non-parabolic Kane valence bands were used in the framework of acoustic phonon scattering dominating:[2]

$$E\left(1+\frac{E}{E_g}\right)=\frac{\hbar^2k^2}{2m^*_{d1}} or \frac{\hbar^2k_l^2}{2m^*_l}+\frac{\hbar^2k_t^2}{2m^*_t}, \backslash^* \text{ MERGEFORMAT (1)}$$

where E_g is the band gap, k and m^* are the wave factors and effective masses along the longitudinal (l) and transversal (t) directions at corresponding energy extrema, and $m^*_{d1} = (m^*_l m^{*2}_t)^{1/3}$ is the effective mass in each single valley. For each single parabolic Kane band, the carrier concentration $n(\varepsilon_F)$ is given by:[2, 3]

$$n(\varepsilon_F)=\frac{(2m^*_d k_B T)^{3/2}}{3\pi^2\hbar^3}\int_0^\infty(\varepsilon+\alpha\varepsilon^2)^{3/2}\left(-\frac{\partial f_0}{\partial\varepsilon}\right)d\varepsilon, \backslash^*$$

MERGEFORMAT (2)

where $\varepsilon = E / k_B T$, $\varepsilon_F = E_F / k_B T$ are reduced charge carrier energy and Fermi energy, f_0 is the Fermi-Dirac distribution function, the value of $\alpha = k_B T / E_g$ represents the band's non-parabolic feature, $m_d^* = N_v^{2/3} m_{d1}^*$ is the density-of-states mass in each band, where N_v is the degeneracy of the band and $m_{d1}^* = (m_l m_t^2)^{1/3}$ the effective mass of each single valley with m_l and m_t as effective masses along the longitudinal and transversal directions respectively.

For light L band,

$m_l = 0.176 \cdot (T / 300)^{1/2} \cdot m_0$,

$m_t = 0.0405 \cdot (T / 300)^{1/2} \cdot m_0$,

For heavy Σ band,

$m_l = m_t = 0.366 \cdot (T / 300)^{1/2} \cdot m_0$,

where m_0 is the mass for an electron unit. The temperature-dependent relation (~ $T^{1/2}$) was adopted following literatures.[4-6]

Correspondingly, in the frame of energy dependent relaxation time approximation,[2] the electrical conductivity σ, Seebeck coefficient S can be expressed as:

$$\sigma = \frac{e^2}{m_I^*} \frac{(2 m_d^* k_B T)^{3/2}}{3\pi^2 \mathrm{h}^3} \left\langle \tau(\varepsilon) \right\rangle, \qquad \text{* MERGEFORMAT (3)}$$

$$S = \frac{k_B}{e} \frac{\left\langle \tau(\varepsilon)(\varepsilon - \varepsilon_F) \right\rangle}{\left\langle \tau(\varepsilon) \right\rangle}, \qquad \text{* MERGEFORMAT (4)}$$

where $m_I = 3(1/m_l^* + 2/m_t^*)^{-1}$ is known as the inertial or conducting effective mass, $\langle x(\varepsilon) \rangle$ is an average of an arbitrary function over energy ε and defined as:

$$\left\langle x(\varepsilon) \right\rangle = \int_0^\infty (\varepsilon + \alpha\varepsilon^2)^{3/2} (1 + 2\alpha\varepsilon)^{-1} \left(-\frac{\partial f_0}{\partial \varepsilon} \right) x(\varepsilon) d\varepsilon \text{ ,* MERGEFORMAT (5)}$$

In the case that acoustic phonons dominates, the corresponding relaxation time is expressed as:[2]

$$\tau_{ac}(\varepsilon) = \left(\varepsilon + \alpha\varepsilon^2\right)^r \left(1+2\alpha\varepsilon\right)^{-1} \frac{2\pi \mathrm{h}^4 C_l}{E_{ac}^2 (2m_{d1}^* k_B T)^{3/2} \left[(1-A)^2 - B\right]}, \backslash^*$$

MERGEFORMAT (6)

where $\varepsilon = E / k_B T$ is the reduced energy, $r = -1/2$ for acoustic scattering, $\alpha = k_B T / E_g$ represents the band's non-parabolic feature, C_l is the combined elastic modulus ($C_l = 58.2$ GPa for SnTe[6]), E_{ac} is the deformation potential of acoustic phonons of each single band (E_{ac_L}=15eV and E_{ac_Σ}=18eV), and $A = \alpha\varepsilon(1-K)/(1+2\alpha\varepsilon)$, $B = 8\alpha\varepsilon(1+\alpha\varepsilon)K/[3(1+2\alpha\varepsilon)^2]$, $K = (E_{ac})_v / (E_{ac})_c$ the ratio of deformation potential between valence and conduction band (K=1.0 is used here).

In the TKB model, the overall Seebeck coefficient, electrical conductivity and Lorenz number are evaluated as follows:

$$S = (S_L \sigma_L + S_\Sigma \sigma_\Sigma)/(\sigma_L + \sigma_\Sigma), \quad \backslash^* \text{ MERGEFORMAT (7)}$$

$$\sigma = \sigma_L + \sigma_\Sigma, \quad \backslash^* \text{ MERGEFORMAT (8)}$$

5. Details of the configurational entropy:

$$\Delta S = -R\sum_{i=1}^{n} x_i \ln x_i \quad \backslash^* \text{ MERGEFORMAT (9)}$$

where k_B and N_A are the Boltzmann constant and Avogadro's number, respectively, R is the gas constant, n is the number of substituted components, and x_i is the mole content of the component.[7]

6. Details of the weighted mobility μ_w and Quality factor *B*:

The temperature-dependent weighted mobility (μ_w) was derived from the experimental electrical conductivity σ and Seebeck coefficient S proposed by G. J. Snyder et al:[8]

$$\mu_W = 331\left(\frac{1}{\rho}\right)\left(\frac{T}{300}\right)^{-\frac{3}{2}}\left[\frac{\exp\left[\frac{|S|}{k_B/e} - 2\right]}{1+\exp\left[-5\left(\frac{|S|}{k_B/e} - 1\right)\right]} + \frac{\frac{3}{\pi^2}\frac{|S|}{k_B/e}}{1+\exp\left[5\left(\frac{|S|}{k_B/e} - 1\right)\right]}\right] \backslash^*$$

MERGEFORMAT (10)

where μ_w is the weighted mobility, ρ is the electrical resistivity measured in mΩ cm, T is the absolute temperature in K, S is the Seebeck coefficient, and k_B/e = 86.3 μV K^{-1}. The formula for calculating the quality factor (B) is as follows:[9, 10]

$$B = 9\frac{\mu_W}{\kappa_{lat}}\left(\frac{T}{300}\right)^{5/2} \qquad \text{* MERGEFORMAT (11)}$$

7. Supplemental Tables

Table. S1 The configurational entropy, ΔS, and the room temperature carrier mobility, μ, carrier concentrations, n, weighted mobility, μ_w, lattice thermal conductivity, κ_l, quality factor, B, of this work involves multi-element co-doping materials.

Samples	ΔS	μ	n	μ_w	κ_l	B
$(SnTe)_{0.85}(Ag_{0.8}Sb_{1.2}Te_{2.2})_{0.15}$	0.75	57.65	1.95	92.3	0.89	0.94
$(Sn_{0.85}Pb_{0.15}Te)_{0.85}$ -$(Ag_{0.8}Sb_{1.2}Te_{2.2})_{0.15}$	1.06	43.48	1.84	77.58	0.83	0.86
$(Sn_{0.8}Pb_{0.15}Ge_{0.05}Te)_{0.85}$ -$(Ag_{0.8}Sb_{1.2}Te_{2.2})_{0.15}$	1.20	37.84	1.73	75.34	0.85	0.81
$(Sn_{0.795}Pb_{0.15}Ge_{0.05}Nd_{0.005}Te)_{0.85}$ -$(Ag_{0.8}Sb_{1.2}Te_{2.2})_{0.15}$	1.22	37.72	1.65	78.97	0.88	0.82
$(Sn_{0.79}Pb_{0.15}Ge_{0.05}Nd_{0.005}In_{0.005}Te)_{0.85}$ -$(Ag_{0.8}Sb_{1.2}Te_{2.2})_{0.15}$	1.25	32.45	1.59	74.73	0.76	0.9

8. Supplemental Figures

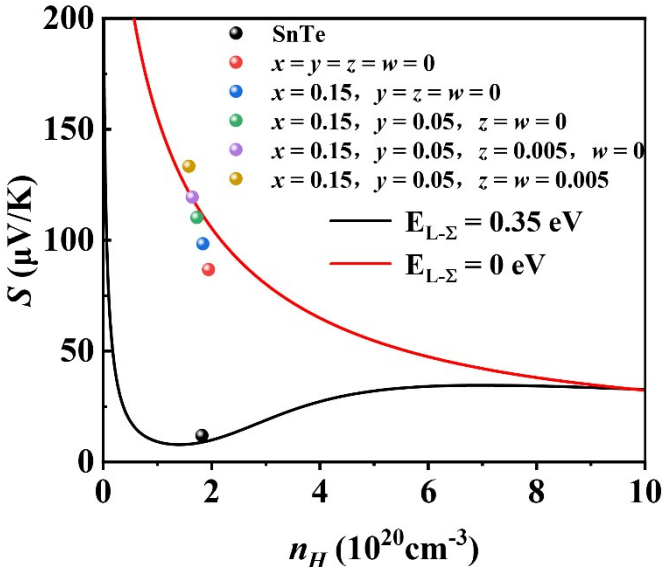

Figure. S1 Experimental Seebeck coefficient (S) as a function of carrier concentration (n_H) *versus* calculated Pisarenko plots via a TBK model with band offsets of 0.35 and 0 eV for SnTe[11] and $(Sn_{1-x-y-z-w}Pb_xGe_yNd_zIn_wTe)_{0.85}(Ag_{0.8}Sb_{1.2}Te_{2.2})_{0.15}$ ($x = y = z = w = 0$; $x = 0.15$, $y = z = w = 0$; x =0.15, $y = 0.05$, $z = w = 0$; $x = 0.15$, $y = 0.05$, $z = 0.005$, $w = 0$; $x = 0.15$, $y = 0.05$, $z = w = 0.005$).

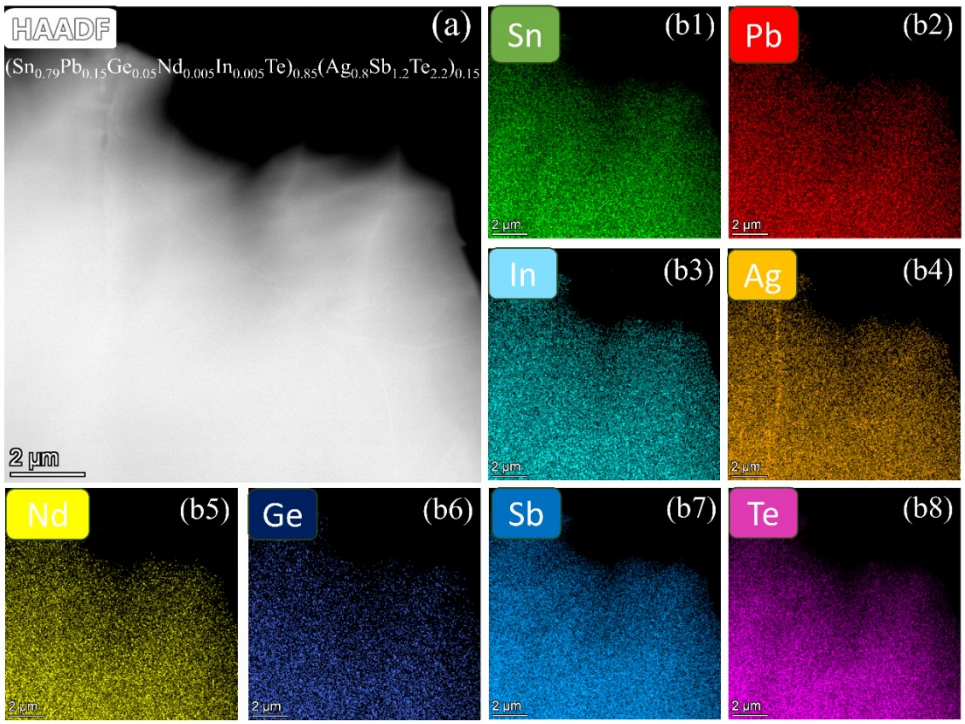

Figure. S2 (a) A HAADF-STEM image and (b) corresponding energy dispersive X-ray spectroscopy (EDS) elemental mappings for $(Sn_{1-x-y-z-w}Pb_xGe_yNd_zIn_wTe)_{0.85}(Ag_{0.8}Sb_{1.2}Te_{2.2})_{0.15}$ ($x = 0.15$, $y = 0.05$, $z = w = 0.005$).

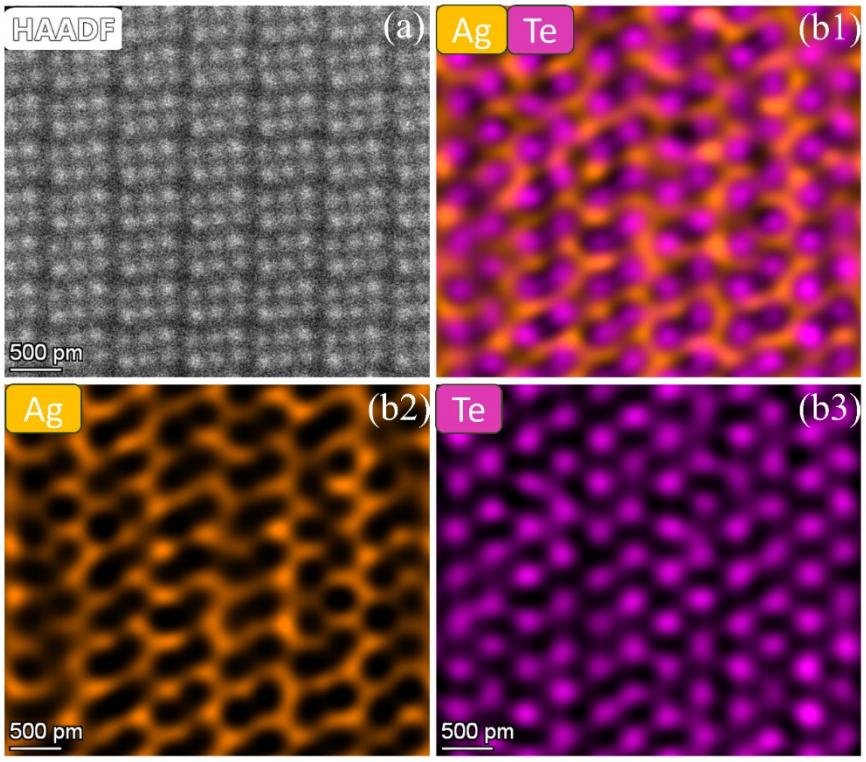

Figure. S3 A atomic-scale HAADF-STEM image and (b) corresponding EDS in the upper left corner of fig 5(b).

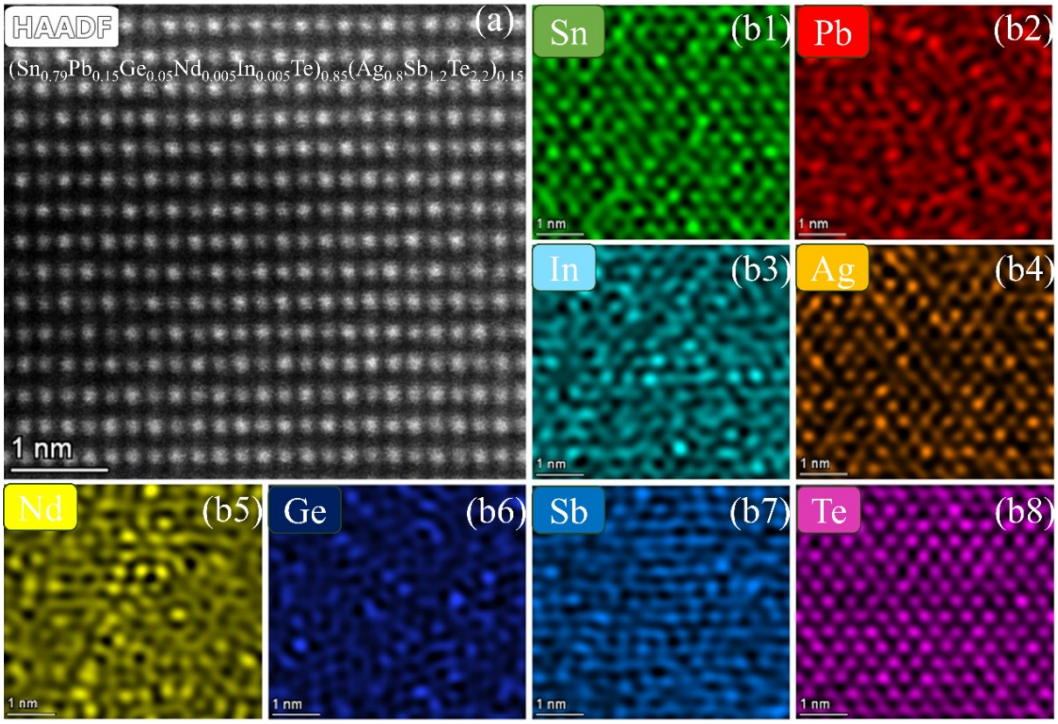

Figure. S4 (a) A atomic-scale HAADF-STEM image and (b1-b8) corresponding EDS elemental mappings for $(Sn_{1-x-y-z-w}Pb_xGe_yNd_zIn_wTe)_{0.85}(Ag_{0.8}Sb_{1.2}Te_{2.2})_{0.15}$ (x = 0.15, y = 0.05, z = w = 0.005).

References

1 R. K. Fitzgerel and F. h. Verhoek, *Journal of Chemical Education*, 1960, **37**, 545-549.

2 S. V. Faleev and F. Léonard, *Phys. Rev. B*, 2008, **77**, 214304.

3 J. P. Heremans, C. M. Thrush and D. T. Morelli, *Phys. Rev. B*, 2004, **70**, 115334.

4 D. Wu, L. D. Zhao, S. Q. Hao, Q. K. Jiang, F. S. Zheng, J. W. Doak, H. J. Wu, H. Chi, Y. Gelbstein, C. Uher, C. Wolverton, M. Kanatzidis and J. Q. He, *J.Am.Chem.Soc.*, 2014, **136**, 11412-11419.

5 Y. Pei, X. Shi, A. LaLonde, H. Wang, L. Chen and G. J. Snyder, *Nature*, 2011, **473**, 66-69.

6 M. Zhou, Z. M. Gibbs, H. Wang, Y. Han, C. Xin, L. Li and G. J. Snyder, *Phys. Chem. Chem. Phys.*, 2014, **16**, 20741-20748.

7 W. Zheng, G. Liang, Q. Liu, J. Li, J. A. Yuwono, S. Zhang, V. K. Peterson and Z. Guo, *Joule*, 2023, **7**, 2732-2748.

8 G. J. Snyder, A. H. Snyder, M. Wood, R. Gurunathan, B. H. Snyder and C. Niu, *Adv. Mater.*, 2020, **32**, 2001537.

9 G. J. Tan, L. D. Zhao and M. G. Kanatzidis, *Chem. Rev.* , 2016, **116**, 12123-12149.

10 R. P. Chasmar and R. Stratton, *Journal of Electronics and Control*, 1959, **7**, 52-72.

11 X. Xu, J. Cui, Y. Yu, B. Zhu, Y. Huang, L. Xie, D. Wu and J. Q. He, *Energy Environ. Sci.*, 2020, **13**, 5135-5142.